

# Improvement of Oil Flowability by Assembly of Comb-Type Copolymers with Paraffin and Asphaltene

Li Li and Jun Xu

State Key Laboratory of Chemical Engineering, East China University of Science and Technology, Shanghai 200237, China

Jack Tinsley

Dept. of Chemical Engineering, Princeton University, Princeton, NJ 08544

Douglas H. Adamson

Dept. of Chemistry, University of Connecticut, CT 06269

Brian A. Pethica, John S. Huang, and Robert K. Prud'homme

Dept. of Chemical Engineering, Princeton University, Princeton, NJ 08544

Xuhong Guo

State Key Laboratory of Chemical Engineering, East China University of Science and Technology, Shanghai 200237, China

DOI 10.1002/aic.12729

Published online July 27, 2011 in Wiley Online Library (wileyonlinelibrary.com).

*Comb-type (maleic acid alkylamides-co- $\alpha$ -octadecene) copolymers (MACs) assemble with long-chain *n*-paraffins and asphaltenes by the hydrophobic alkyl branches and polar groups, respectively, and improve flowability of crude oils upon cooling. Their effects on the crystallization of paraffins from model oils were studied by rheology, optical microscopy, differential scanning calorimetry, and X-ray diffraction. Upon cooling, MACs change the size and shape of paraffin crystals and reduce the yield stresses of gels generated by precipitated solids. Deposition of wax was significantly suppressed by MAC as observed using a laboratory-scale deposition apparatus. MACs are more effective than poly(ethylene-butene) copolymers in improving the flowability of crude oils containing asphaltenes. The interactions between the carboxyl and amide groups of MAC with the polar aromatic asphaltenes appear to stabilize crudes through the steric effects of the long alkyl groups of MAC polymers, thereby reducing the strength of paraffin/asphaltene gels formed on cooling. © 2011 American Institute of Chemical Engineers AICHE J, 58: 2254–2261, 2012*

**Keywords:** crude oil, flowability, paraffin, asphaltene, comb polymer

## Introduction

Crude oils mainly consist of paraffins, aromatic hydrocarbons, resins, and asphaltenes. In deep oil well with high temperature, they behave as Newtonian fluids with low viscosities, while the solubility of long-chain paraffins and asphaltenes decreases sharply at lower temperatures in pipelines.<sup>1</sup> The resulting dispersion of long-chain paraffin solids and asphaltenes can lead to deposition at the pipe walls, reducing oil flow and even blocking the pipeline.<sup>2</sup> This problem can be more serious for offshore deep-sea wells where the temperature at the sea bed can be 4°C. The remediation of plugged pipelines in water depths of 400 m can cost \$1 million/mile as reported by the U.S. Department of Energy.<sup>3</sup> To manage the wax deposition problem, thermal, mechanical (pigging), and chemical (wax inhibitor) methods are avail-

able. Polymers for wax inhibition and deposition control play an important role in the field of "flow assurance."

Copolymers with crystalline/amorphous diblock structures such as ethylene-vinyl acetate copolymer,<sup>4,5</sup> polyethylene-poly(ethylenepropylene),<sup>6</sup> poly(ethylene-butene) (PEB),<sup>7–12</sup> and poly(maleic anhydride-co- $\alpha$ -olefin)s esterified by alkyl alcohols<sup>13,14</sup> are reported to be able to improve the cold flow of waxy oils by modifying paraffin crystallization. Further improvement in efficacy is the aim of much current research.<sup>15–17</sup>

In this work, we synthesized comb-type (maleic acid alkylamides-co- $\alpha$ -octadecene) copolymers (MACs) by amidation of maleic anhydride/ $\alpha$ -olefin copolymers with *n*-alkylamines of carbon number of 12, 14, or 18. Their effects on the crystallization of long-chain paraffins and the flowability of model and crude oils (with and without asphaltenes) upon cooling were examined using the methods of rheology, optical microscopy, differential scanning calorimetry, X-ray diffraction, and a developed laboratory-scale deposition system to correlate MAC structure, wax crystal structure, flowability, and deposition.

Correspondence concerning this article should be addressed to R. K. Prud'homme at prudhomm@princeton.edu., and X. Guo at guoxuhong@ecust.edu.cn.

Table 1. Crude Oil Components

Crude oil	Paraffin (wt %)	Asphaltenes (wt %)	Source
CO-1	5	0.4	Halliburton
CO-2	10	0.4	Halliburton
CO-3	3	0.2	Tomark Industries

## Experimental

### Materials

Decane (anhydrous, 99+%), maleic anhydride (99%), 1-octadecene (95%), benzoyl peroxide (97%), *o*-xylene (98%), octadecylamine (97%), tetradecylamine (98%), dodecylamine (98%), octacosane (C28, >99%, F.W. 394.77, m.p. 59°C), dotriacontane (C32, >97%, F.W. 450.88, m.p. 69°C), hexatriacontane (C36, >98%, F.W. 506.99, m.p. 74–76°C), and two mixed wax (Aldrich number 32724 with a melting point from 53 to 57°C and Aldrich number 411663 with a melting point 65°C) were purchased from Aldrich and were used as obtained. The solvent Norpar 12 Fluid (a mixture of normal alkanes from C10 to C14) was obtained from ExxonMobil Corporation.

Model waxy oil samples were prepared by dissolving C28, C32, or C36 *n*-alkanes in decane and heating at 20°C/min to 70°C, above the melting temperature of waxes. The samples were held at that temperature for 5 min. Solid crystal samples were then prepared by cooling the model waxy oils from 70 to 0°C at the rate of 1°C/min and separating the precipitated crystals by filtration with vacuum in an ice bath and drying under vacuum at room temperature for 3 days. Crystal samples were sealed and stored at about –4°C before using. Three crude oils used in this work are described and listed in Table 1. Asphaltene content was measured by weighing the precipitate formed after addition of *n*-heptane at laboratory temperature. Paraffin content was estimated as the precipitate formed after addition of acetone and cooling to 0°C.

Microcrystalline random copolymers PEBs were prepared following the method reported previously.<sup>7</sup> The final polymers had molecular weights of about 7000 g/mol and a distribution of molecular weight of about 1.03. Two PEBs (PEB7.5 and PEB10) were used, where the number denotes the ethyl side branches per 100 backbone carbons as determined via <sup>1</sup>H NMR. PEB with hydroxyl grafts (PEB7.5-OH) was synthesized as reported previously.<sup>18</sup>

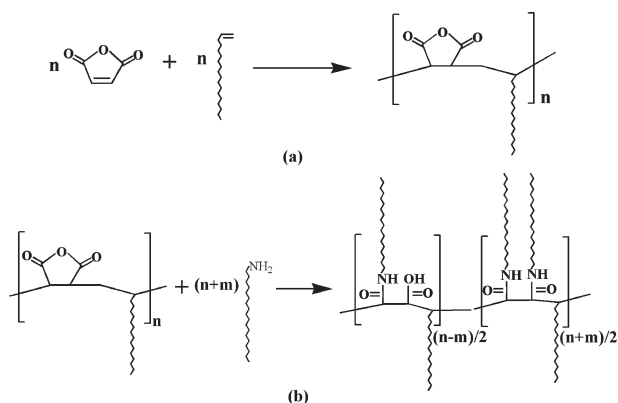


**Figure 1. Synthesis of (a) maleic anhydride-co- $\alpha$ -olefin polymer and (b) maleic acid alkylamides-co- $\alpha$ -octadecene copolymers (MAC).**

Table 2. Characterization of MACs

Polymer	Molecular weight (kg/mol)	Molecular weight distribution	Amidation ratio <i>f</i>
MAC18-18	11.2	1.5	1.4
MAC18-14	11.5	1.5	1.5
MAC18-12	12.3	1.4	1.4

### Synthesis of MAC

(Maleic anhydride-co- $\alpha$ -octadecene) polymer was copolymerized from  $\alpha$ -octadecene and maleic anhydride in *o*-xylene using benzoyl peroxide as initiator (Figure 1a). By amidation with excess octadecylamine, tetradecylamine, or dodecylamine (Figure 1b), the comb-type (maleic acid alkylamides-co- $\alpha$ -octadecene) copolymers (defined as MAC18-18, MAC18-14, and MAC18-12, respectively) were obtained.

In a typical run, 1-octadecene and maleic anhydride were dissolved in *o*-xylene and benzoyl peroxide dissolved in *o*-xylene was gradually added to the reactants. Heated to about 125°C, the mixture was refluxed with vigorous stirring for 2 h. The polymeric product was then reacted with determined amount of octadecylamine at about 110°C for 12 h. Purification of the raw products was carried out by pouring in an excess volume of methanol, followed by filtration and vacuum drying. Their molecular weights and molecular weight distributions were determined by gel permeation chromatography (GPC) using polystyrene samples as standards. The results are listed in Table 2.

The amidation ratio (*f*) gives the number of alkylamides (between one and two) formed for each maleic group of the polymer, estimated from the integrated areas of peaks at around 0.88 ppm for the chain terminal methyl protons ( $A_{CH_3}$ ) and 3.28 ppm for the three protons singly linked to carbon in each maleic group ( $A_{CH}$ )<sup>19–22</sup>:

$$\frac{A_{CH}}{A_{CH_3}} = \frac{2}{3 + 3f}, \quad f = \frac{2A_{CH_3}}{3A_{CH}} - 1$$

The results are listed in Table 2. It will be noted that the MAC used in this study have approximately one residual carboxyl group per two maleic acid units, possibly distributed randomly.

### Yield stress measurement

The yield stress ( $\tau_y$ ) is defined as the stress below which no flow occurs. An operational definition of  $\tau_y$  was adopted as the stress at the transition between the creep and liquid-like viscosity regimes where  $\tau_y$  can be identified as the stress for which the derivative is a maximum.<sup>6</sup> The yield stress measurements were performed on a MCR501 rheometer by Anton-Paar Physica (Graz, Germany) that equipped with parallel-plate geometry. The temperature of the lower surface was controlled to within 0.1°C by a Peltier plate, and a hood with a Peltier heating device was used to heat the parallel plate and limit evaporation of the solvent. With the model oils (long-chain *n*-paraffins in decane solution) the samples were initially heated to 70°C, kept at this temperature for 5 min to erase their thermal history and then cooled to the experimental test temperature of 0°C at a rate of ca. 20°C/min. With the crude oils, the cooling stage was cooled to form the gels for stress testing. After allowing the sample to anneal at constant temperature under no stress for 20 minutes, a stress was applied and incrementally increased

every 10 seconds (100 stress increments per decade) and the viscosity measured. The initial applied stress was chosen well below the stress at which creep begins.

### Optical microscopy

Wax crystal morphologies were observed using a Nikon TE200 inverted microscope with phase and differential interference contrast (DIC) optics (Micron Optics, Cedar Knoll, NJ). Images were captured using a Kodak ES 310 charge coupled device (CCD) camera connected to a personal computer (PC) via a name of a video capture card (PIXCID) imaging board (EPIX, Buffalo Grove, IL). A small quantity of waxy oil was transferred from storage at  $-4^{\circ}\text{C}$  directly to a glass slide inside a copper stage with a central window for observation. The temperature of the copper stage was controlled at  $0^{\circ}\text{C}$  by a circulating bath. Images were taken at five sites on the slides.

### Differential scanning calorimetry

The differential scanning calorimeter is a Perkin-Elmer (Norwalk, CT) Pyris differential scanning calorimetry (DSC) 7. The temperature scale was calibrated by the melting temperature of ice from deionized (DI) water and the heat flow by the fusion of an indium standard. An empty stainless steel sample pan was used as the reference, and the baseline was established by running an empty pan before the sample measurement. About 10 mg model waxy oil was weighed into a pan and hermetically sealed. The pan was then placed into the DSC sample tray. Scanning rates ranged from 1 to  $10^{\circ}\text{C}/\text{min}$ , and the temperature ranges were chosen to ensure that the base line was stable for at least  $10^{\circ}$  before the first peak and after the last peak. The calorimeter chamber was continuously purged with dry nitrogen. The enthalpies of crystallization and melting of paraffins were calculated from the peak areas using the Pyris software. Regular sampling showed no weight loss from the hermetically sealed sample pans.

### X-ray scattering

One-dimensional images were collected in the reflection mode from dried samples of long-chain *n*-paraffin crystals at room temperature using an evacuated Statton camera manufactured by Philips-Norelco. The crystals were held on glass slides with double-layer tape (Winmore, Frank W. Winne & Son, Inc., PA). The slides were arranged with their planes orthogonal to the plane of the X-ray source, sample, and detector. Detector and sample were synchronously rotated. X-rays with a source wavelength of 0.154 nm were produced using a sealed tube generator with a Cu target and a Huber graphite monochromator. The scattering patterns were recorded over the range of angles corresponding to  $2\theta$  from  $1.5$  to  $50^{\circ}$ . The background diffraction (tape and slide) was subtracted from the raw spectra gave the 1D X-ray diffractograms of paraffin crystals.

### $^1\text{H}$ NMR spectra

The proton spectra of MAC were recorded on a Varian Inova-400 NMR spectrometer operating at 400 MHz for protons at room temperature.

### Deposition experiment

Deposition tests were performed by passing warm model waxy oils over a cold surface through a laboratory-scale loop. A parallel-plate cell consisting of a copper bottom plate with cooling water channel and a transparent poly (methyl methacrylate) upper plate was used. The increase in

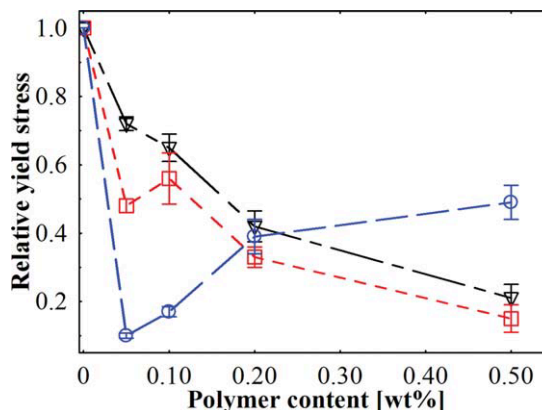


**Figure 2.** Relative yield stresses (defined as ratio of yield stress with polymer to that without polymer) of model waxy oil 4%C36 as a function of MAC content.

Symbols denote: (○) MAC18-18; (□) MAC18-14; and (▽) MAC18-12. [Color figure can be viewed in the online issue, which is available at [www.interscience.wiley.com](http://www.interscience.wiley.com).]

pressure, which was related to a change in the average channel height, was measured by pressure taps placed over the flow path in and out the cell. An external loop consisted of a section to reheat the model waxy oils to fully dissolve any precipitated wax, a pump, and a heat exchanger to bring the model oils entering the cell to a determined temperature.<sup>23,24</sup>

## Results and Discussion

### Effect of MAC on paraffin crystallization

Figure 2 shows that the yield stresses of the gels formed on cooling 4% C36 solutions in decane were reduced by addition of each MAC. The yield stress decreased almost monotonically with concentration of MAC18-12 and MAC18-14 while a minimum with the lowest yield stress observed was found for MAC18-18 at 0.05 wt %. For the C36 model oil, MAC18-18 is most effective in improving the cold flow. The increase of the yield stress at higher MAC18-18 concentrations may be due to a polymer-bridging effect between the paraffin crystals.<sup>8,9</sup> MAC18-18 also reduces the yield stresses of the cooled 4% C32 and C28 model waxy oils, being most effective for 4%C28 (Figure 3).

However, the ability of the MAC polymers to reduce the yield stresses of these model waxy oils compares unfavorably with PEB,<sup>7,8</sup> as shown in Figure 4. The yield stress of 4%C32 can be reduced by three to four orders of magnitude by PEB7.5 or PEB10 as compared to only one order for MAC18-18 (Figure 4).

As observed by optical microscopy (Figure 5), the sizes of C36 crystals from 4 wt % solutions in decane at  $0^{\circ}\text{C}$  were reduced by MAC18-18, MAC18-14, or MAC18-12, and the shapes changed significantly from large plate-like crystals to spindle shapes or particles of indistinct geometry. Higher content of MAC leads to smaller crystal sizes (Figures 5b, c and e, f). MAC18-18 reduces the C36 crystals to smaller sizes than MAC18-14 or MAC18-12 (Figures 5b, d, e). These observations are consistent with the rheological results in that crystal size and platelet shape correlate qualitatively with the yield stress of cooled model waxy oil.

Further insight on the influence of MAC on paraffin crystallization from the model waxy oils is obtained from DSC.



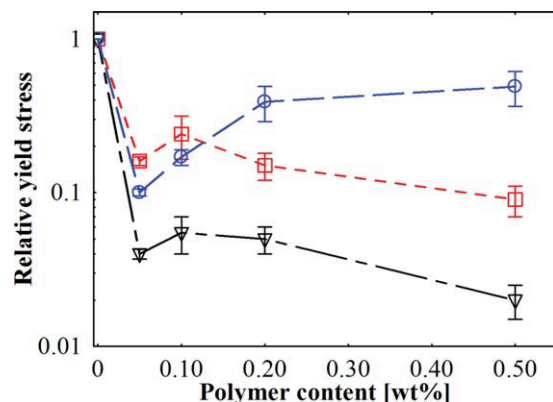


**Figure 3. Relative yield stresses of model waxy oils as a function of polymer MAC18-18 content.**

Symbols denote: (○) 4%C36; (□) 4%C32; and (▽) 4%C28. [Color figure can be viewed in the online issue, which is available at [wileyonlinelibrary.com](http://wileyonlinelibrary.com).]

As shown in Figure 6, addition of MACs broadens the phase transition peaks upon cooling and moves the onset of paraffin crystallization to slightly lower temperatures with a parallel trend to lower enthalpies of the transitions. These effects follow the sequence MAC18-18 > MAC18-14 > MAC18-12 at 0.1% polymer concentration. These changes in onset temperature and crystallization enthalpy increase with concentration of MAC18-18 (Figure 7). The monotonic decrease in  $T_{\text{onset}}$  and crystallization enthalpy upon addition of MAC18-18 observed by DSC reflects the cocrystallization and assembly of MAC18-18 with paraffins. MAC18-18 molecules assemble on the surface of paraffin crystals which inhibits the growth of crystal size upon cooling model waxy oils. More MAC18-18s lead to less paraffin crystals, smaller crystal size and delayed crystallization upon cooling. The trend of these DSC results correlates with the optical microscopy observations (Figure 5).

Figure 8 shows the X-ray scattering patterns of C36 crystal samples from decane solutions with and without addition of MAC. The crystal morphologies of C36 from decane in the absence of polymers are large and plate-like (Figure 5a). The plate-like crystals will tend to be in preferred orientation parallel to the support. As the support and detector are rotated in one plane with the stationary radiation source, these platelet samples should show the low-angle scattering well. High-angle scattering will show up increasingly with smaller and less plate-like crystals. These effects are observed, as shown in Figure 8: MACs reduce the low-angle scattering from the layered structure of the paraffin crystals in the sequence MAC18-18 > MAC18-14 > MAC18-12. Increasing the MAC18-18 content eliminates the ordered low-angle scattering and intensifies the two high-angle scattering around 22 and 24° (2θ) from the monoclinic unit cell, correlating with the observations by optical microscope (Figure 5). The contribution of MACs themselves to the X-ray scattering intensity should be negligible, because all the three MAC samples are mostly amorphous. We hypothesize that the alkyl chains in MAC molecules cocrystallize from decane with the long-chain *n*-paraffins, inhibiting platelet formation and the growth of large crystals.<sup>25</sup> The changes induced in crystal shape and size, together with the presence of polymer at the crystal interfaces, can account both for the

effect of MAC on the yield stresses of the gels produced on cooling and for the changes in the DSC properties of the separated solids.

Deposition experiments were performed in a relatively high wall shear stress regime of 60–90 Pa with the channel height of 0.18 mm, flow rate of 325 mL/min, and the Reynolds number of 320. The mixed wax consisting of 55 wt % Aldrich wax number 327204 and 45 wt % Aldrich wax number 411663 (with a carbon number 20–30 as determined by gas chromatography (GC))<sup>23</sup> was dissolved in Norpar 12 with a concentration of 3 wt %. All tests were run with the temperature of the copper plate at 21.4°C, and the temperatures of the model oil inlet at 30.4°C. As shown in Figure 9, the addition of 0.1 wt % MAC18-18 prevented the deposition of wax from model waxy oil significantly.

#### Effect of PEB and MAC polymers on crude oils

The yield stresses of the gels formed by cooling crude oils from 70°C to a range of lower temperatures were measured with and without addition of comb-type polymers. For crude oil CO-1 (containing 5% paraffins and 0.4% asphaltenes), the yield stresses at 0°C were reduced by up to four orders of magnitude by addition of MAC18-18, whereas by only one order with PEB (Figure 10a). The yield stress decreases significantly with concentration of MAC18-18 up to 0.1% (Figure 10a, one point only) while increasing PEB10 content shows minor impact on the yield stress (Figure 10a). Even for CO-2 with a high paraffin content of 10% and the same asphaltene content as CO-1, MAC18-18 is far more effective than PEB in reducing the yield stress (Figure 10b).

To further explore the effect of asphaltenes on cold flow of crude oils, we observed the behavior of CO-3 with 3% paraffin and 0.2% asphaltenes under the influence of MACs and PEBs (Figure 11). MACs are also more effective than PEB7.5 in reducing the yield stresses of the gels formed on cooling CO-3 with lower paraffin and lower asphaltene content. Again, MAC18-18 is more effective than the other MACs, with MAC18-12 the least effective. As shown in Figure 11, PEB7.5 is less effective than all MACs to reduce the yield stress of CO-3. But, however, PEB7.5-OH is significantly better than PEB7.5 to reduce the yield stresses of CO-3. It means that the introduction of polar hydroxyl

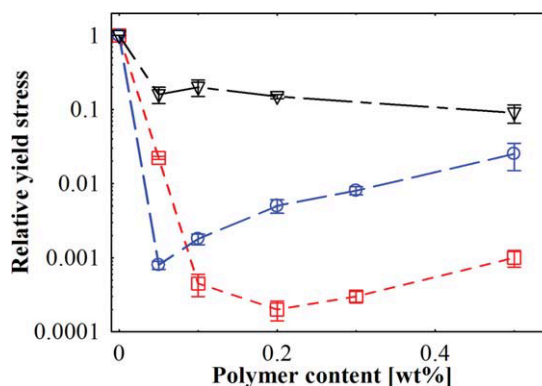


**Figure 4. Relative yield stresses of model waxy oil 4%C32 as a function of polymer contents.**

Symbols denote: (○) PEB7.5; (□) PEB10; and (▽) MAC18-18. [Color figure can be viewed in the online issue, which is available at [wileyonlinelibrary.com](http://wileyonlinelibrary.com).]

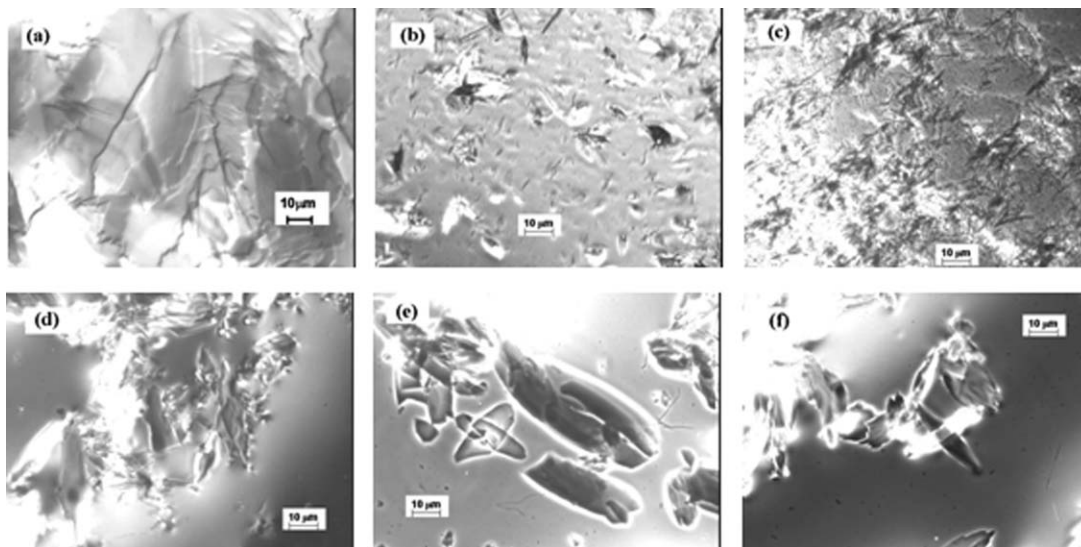


**Figure 5. Optical micrographs of crystals from 4 wt % hexatriacontane (C36).**

(a) C36; (b) C36 + 0.05%MAC18-18; (c) C36 + 0.5%MAC18-18; (d) C36 + 0.05%MAC18-14; (e) C36 + 0.05%MAC18-12; and (f) C36 + 0.5%MAC18-12.

groups into PEB7.5 can improve its effect on flowability improvement for crude oil with asphaltenes.

Comparing the effects of the polymers tested on crude oils, MAC18-18 gives better yield stress reduction than the shorter chain length MACs, with the superior effect greater with increasing at higher asphaltene content and MAC18-18 concentration (Figures 9a and 10a). The interactions between MAC18-18 and asphaltenes appear to play an important role in improving cold flow of crude oils. For the crude oils, both PEB polymers tested give modest decreases in the cooled gel yield strengths, comparable to the MAC18-12 and MAC18-14. MAC18-18 was superior to PEBs in reducing yield strengths for all four crude oils, with the smallest advantage over PEBs shown with the high paraffin, no asphaltene CO-4, approximating the findings with the model oils comprising pure paraffins in decane with no asphaltenes.

Crude oil samples with and without MAC or PEB were observed by polarized-light microscopy. The solids from CO-1 and CO-2 on cooling without addition of polymers

(Figure 12) are predominantly plate-like, but smaller than the crystals from the model oils (Figure 5). As shown in Figure 12, both MACs and PEBs reduce the size of the particles from crude oils CO-1 and CO-2 upon cooling, with MAC18-18 more effective than PEB10 and PEB7.5. The crystal sizes become smaller when MAC18-18 content increases from 0.01% to 0.1% (Figures 12a2, a3). The solids formed from CO-3 and CO-4 on cooling in the absence of polymers are strikingly different to those from the other crude oils and the model oils. The “crystals” are small with indistinct morphologies (Figures 12c, d). Addition of MAC18-18 appears to reduce crystal size further for both CO-3 and CO-4, but this trend is not found with MAC18-12 and MAC18-14 in these two crude oils. The particle sizes and morphology of the solids from the nonasphaltinic high paraffin CO-4 are particularly noteworthy, in sharp contrast with the crystals from the model oils. The results given in Figure 12 show that the qualitative correlation between the formation of large plate-like crystals and the yield strength of the gels formed on cooling the model oils carries over to at least two

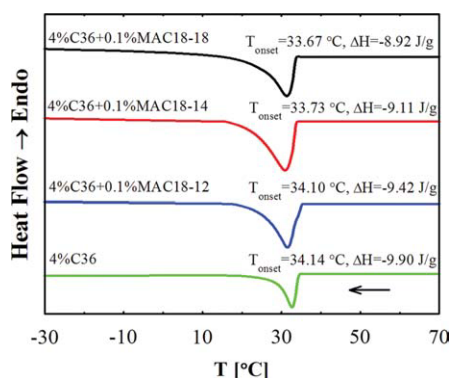


**Figure 6. DSC thermographs of crystals from 4 wt % C36 in decane with and without addition of 0.1% of MAC18-18, MAC18-14 or MAC18-12 during cooling at 10° C/min.**

[Color figure can be viewed in the online issue, which is available at [wileyonlinelibrary.com](http://wileyonlinelibrary.com).]

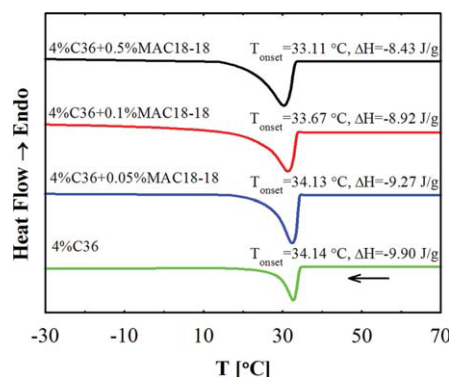


**Figure 7. DSC thermographs of crystals from 4 wt % C36 in decane with addition of different amount of MAC18-18 during cooling at 10° C/min.**

[Color figure can be viewed in the online issue, which is available at [wileyonlinelibrary.com](http://wileyonlinelibrary.com).]

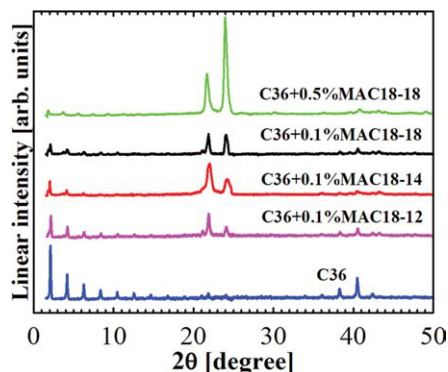


**Figure 8.** One-dimensional X-ray reflection diffractograms for crystals from 4% C36 solutions in decane with and without addition of MACs.

[Color figure can be viewed in the online issue, which is available at [wileyonlinelibrary.com](http://wileyonlinelibrary.com).]

of the crude oils (CO-1 and CO-2) tested. The results for the nonasphaltic crude CO-4 and the crude CO-3 with low content of both paraffins and asphaltenes show that the effect of MACs on cold flow properties will still depend on the complex composition of crudes.

It is well recognized in oilfield practice that the aggregation of asphaltenes from crude oil aggravates wax deposition problems.<sup>15,26–29</sup> Asphaltenes are the heaviest and most polar fraction of crude oil. They are generally composed of polyaromatics carrying aliphatic chains or rings with polar groups containing sulfur, oxygen, and nitrogen, and metals elements such as vanadium and nickel also present.<sup>22</sup> Asphaltenes can be stabilized using polymer amphiphiles by forming a steric polymer layer around the asphaltene particles.<sup>26–29</sup> With their residual carboxyl groups and long alkyl grafts, MACs are amphiphilic. The reduction in the yield stress of cooled asphaltic crude oils by MACs, most effectively by MAC18-18, results not only from the modification of paraffin crystallization but also from asphaltene stabilization. It appears that MAC molecules assemble on the surface of asphaltene particles to form a steric layer and thus, inhibit the asphaltene aggregation in crude oils upon cooling (Figure 13).

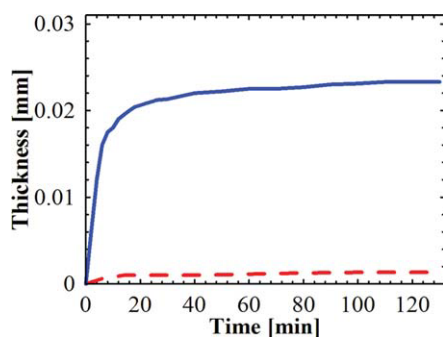


**Figure 9.** Growth of the deposit height with time for a 3 wt % mixed wax solution with (dashed line) and without (solid line) polymer additive MAC18-18.

[Color figure can be viewed in the online issue, which is available at [wileyonlinelibrary.com](http://wileyonlinelibrary.com).]

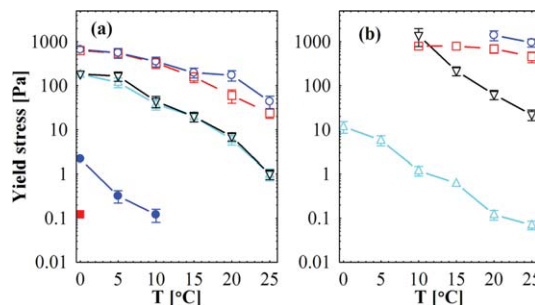


**Figure 10.** Effect of polymers on the yield stress of gels formed on cooling crude oils to a range of temperatures.

(a) CO-1. Symbols denote: (○) CO-1, (□) CO-1 + 0.1%PEB7.5, (▽) CO-1 + 0.01%PEB10, (Δ) CO-1 + 0.1%PEB10, (●) CO-1 + 0.01%MAC18-18, and (■) CO-1 + 0.1%MAC18-18 (one point only). (b) CO-2. Symbols denote: (○) CO-2, (□) CO-2 + 0.1%PEB7.5, (▽) CO-2 + 0.1%PEB10, and (Δ) CO-2 + 0.1%MAC18-18. The yield stress for CO-2 at 0°C is off-scale of the rheometer. [Color figure can be viewed in the online issue, which is available at [wileyonlinelibrary.com](http://wileyonlinelibrary.com).]

As shown in Figure 13, two kinds of molecular assemblies contribute to the improvement of flowability of crude oils on cooling. The nonpolar side alkyl chains in MACs can cocrystallize with long-chain paraffins to anchor into paraffin crystals while the other parts of MAC molecules form a brush-like layer to control the crystal size. In terms of asphaltenes in crude oils, the polar carboxyl groups and amide linkages in MACs can disperse them and prevent them from aggregation.

It is worth noting that the composition of crude oils varies significantly with their sources. An optimized MAC structure that includes both crystallization and polar interactions is required—for these experiments, the MAC18-18 was most effective for oils used in this work. The advantages of using these comb-type MACs as cold flowing improvers for crude oils are that the side alkyl chain lengths can be readily altered during amidation and the polarity of functional groups along the backbone can be varied by the degree of amidation. Therefore, structure can be tuned to oil type.

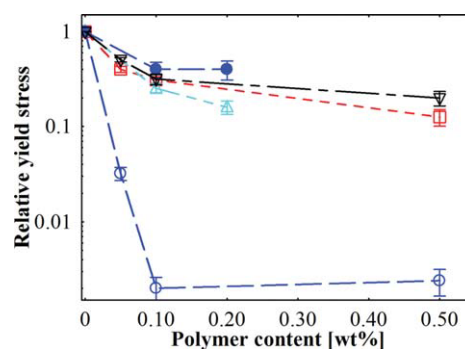


**Figure 11.** Relative yield stresses as a function of polymer contents for crude oils CO-3.

Symbols denote: (●) CO-3 + 0.1%PEB7.5, (▽) CO-3 + 0.1%MAC18-12; (□) CO-3 + 0.1%MAC18-14, (Δ) CO-3 + 0.1%PEB7.5-OH, (○) CO-3 + 0.1%MAC18-18. [Color figure can be viewed in the online issue, which is available at [wileyonlinelibrary.com](http://wileyonlinelibrary.com).]



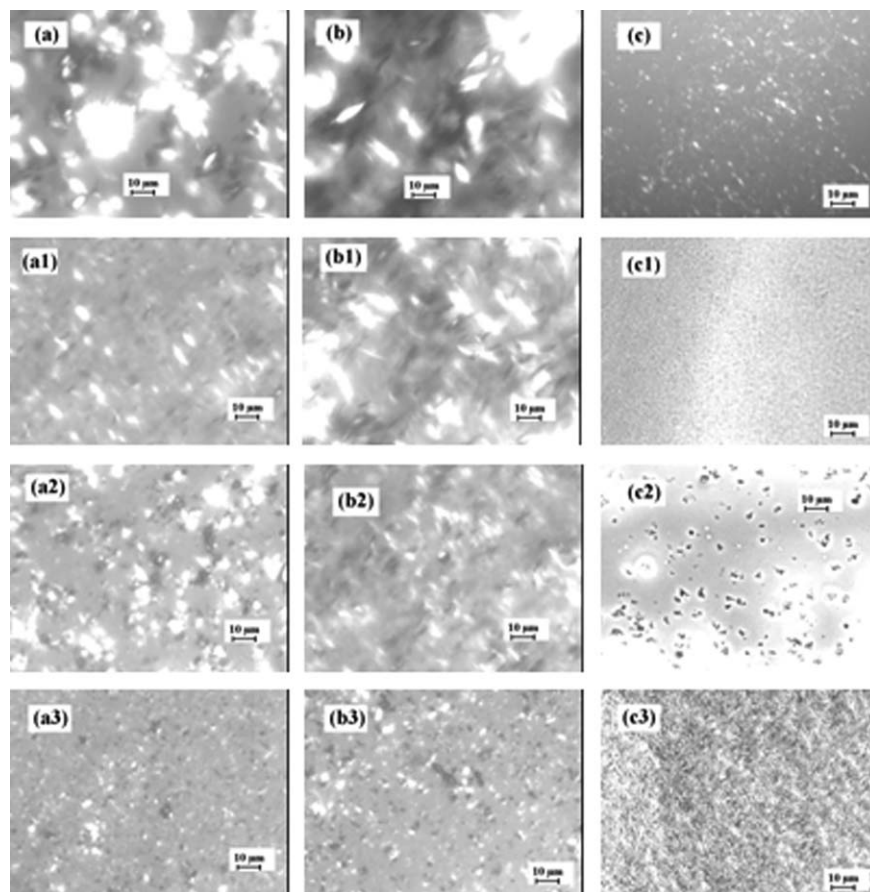


**Figure 12. Optical micrographs of crude oils with and without MACs at 0°C.**

(a) CO-1; (a1) CO-1 + 0.1% PEB10; (a2) CO-1 + 0.01% MAC18-18; (a3) CO-1 + 0.1% MAC18-18; (b) CO-2; (b1) CO-2 + 0.1% PEB10; (b2) CO-2 + 0.1% PEB7.5; (b3) CO-2 + 0.1% MAC18-18; (c) CO-3; (c1) CO-3 + 0.1% MAC18-18; (c2) CO-3 + 0.1% MAC18-14; (c3) CO-3 + 0.1% MAC18-12.

## Conclusions

Comb-type (maleic alkylamide-co- $\alpha$ -octadecene) copolymers (MACs) were synthesized by the amidation of poly (maleic anhydride-co- $\alpha$ -octadecene) by alkyl amines. These copolymers reduce the yield stresses of the gels formed on cooling model waxy oils made up of long-chain paraffins (C28, 32, and 36) in decane. They also decrease the paraffin crystal sizes, suppress the formation of crystal platelets, and lower the paraffin crystallization temperatures and enthalpies. MACs prevent the deposition of wax from solution upon cooling significantly as observed using a developed laboratory-scale deposition system.

MAC is more effective than PEBs in improving cold flow of crude oils containing asphaltenes. The size of the plate-like precipitated particles formed on cooling two crude oils (CO-1 and CO-2) is significantly reduced by addition of MAC, and platelet formation is inhibited. The solids formed in the absence of polymers from the other two crudes tested (CO-3 and CO-4) comprised small crystals and indefinite morphology, and the effect of MAC addition depends on the side-chain length. The qualitative correlation of platelet formation and crystal size with the yield stress found for the gels from cooled model oils does not carry over to some crude oils. The results with the nonasphaltic crude CO-4 indicate that the particular compositions of the “paraffins” as assayed by precipitation with acetone are relevant to cold flow and its modification by polymers. With the crudes con-

taining asphaltenes, MAC18-18 is clearly the best polymer tested in this experimental series. It is hypothesized that MAC18-18 interacts as a polar amphiphile with the aromatic and polar asphaltenes to reduce asphaltene coagulation and coprecipitation with the paraffins.

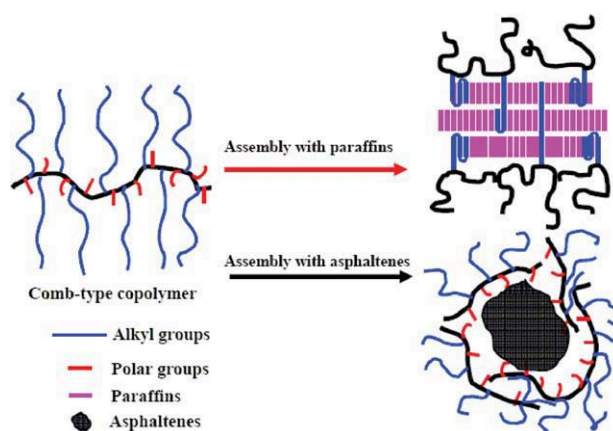


**Figure 13. Schematic representation of comb-type copolymer assembly in crude oil on asphaltene precipitates.**

The precipitates may be either in solution or deposited on the wax crystal surface. [Color figure can be viewed in the online issue, which is available at [wileyonlinelibrary.com](http://wileyonlinelibrary.com).]

## Acknowledgments

We thank Halliburton Energy Services Inc., the National Natural Science Foundation of China (Grant Nos. 20774028, 51003030, and 51003028), the 111 Project Grant B08021, the Fundamental Research Funds for the Central Universities, the Key Basic Research Project of Shanghai Science and Technology Commission (10JC1403800), and the Scientific and Technological Project of Shanghai Science and Technology Commission (10111100103) for support of this study.

## Literature Cited

1. Singh P, Venkatesan R, Fogler HS, Nagarajan NR. Morphological evolution of thick wax deposits during aging. *AIChE J.* 2001;47:6–18.
2. Ribeiro FS, Mendes PRS, Braga SL. Obstruction of pipelines due to paraffin deposition during the flow of crude oils. *Int J Heat Mass Transfer.* 1997;40:4319–4328.
3. Paso KG, Fogler HS. Bulk stabilization in wax deposition systems. *Energy Fuels.* 2004;18:1005–1013.
4. Gilby GW. The use of ethylene-vinyl acetate copolymers as flow improvers in waxy crude oil. Special Publication-Royal Society of Chemistry. *Chem Oil Ind.* 1983;45:108–124.
5. Ashbaugh HS, Guo XH, Schwahn D, Prud'homme RK, Richter D, Fetters LJ. Interaction of paraffin wax gels with ethylene/vinyl acetate copolymers. *Energy Fuels.* 2005;19:138–144.
6. Ashbaugh HS, Fetters LJ, Adamson DH, Prud'homme RK. Flow improvement of waxy oils mediated by selfaggregating partially crystallizable diblock copolymers. *J Rheol.* 2002;46:763–776.
7. Ashbaugh HS, Radulescu A, Prud'homme RK, Schwahn D, Richter D, Fetters LJ. Interaction of paraffin wax gels with random crystalline/amorphous hydrocarbon copolymers. *Macromolecules.* 2002;35:7044–7053.
8. Guo XH, Pethica BA, Huang JS, Prud'homme RK, Adamson DH, Fetters LJ. Crystallization of mixed paraffin from model waxy oils and the influence of micro-crystalline poly(ethylene-butene) random copolymers. *Energy Fuels.* 2004;18:930–937.
9. Guo XH, Pethica BA, Huang JS, Prud'homme RK. Crystallization of long-chain *n*-paraffins from solutions and melts as observed by differential scanning calorimetry. *Macromolecules.* 2004;37:5638–5645.
10. Guo XH, Pethica BA, Huang JS, Adamson DH, Prud'homme RK. Effect of cooling rate on crystallization of model waxy oil with micro-crystalline poly(ethylene butane). *Energy Fuels.* 2006;20: 250–256.
11. Tinsley JF, Prud'homme RK, Guo XH, Adamson DH, Callahan S, Amin D, Shao S, Krigel R, Saini R. Novel laboratory cell for fundamental studies of the effect of polymer additives on wax deposition from waxy oils. *Energy Fuels.* 2007;21:1301–1308.
12. Tinsley JF, Jahnke JP, Adamson DH, Guo XH, Amin D, Krigel R, Saini R, Dettman HD, Prud'home RK. Waxy gels with asphaltenes 2: use of wax control polymers. *Energy Fuels.* 2009;23:2065–2074.
13. El-Gamal IM, Gad EAM, Faramawi S, Gobieli S. Flow improvement of waxy western desert gas oil. *J Chem Technol Biotechnol.* 1992;55:123–130.
14. Son AJ, Graugnard RB, Chai BJ. The effect of structure on performance of maleic anhydride copolymers as flow improvers of paraffinic crude oil. *SPE Int Symp Oilfield Chem.* 1993;SPE25186:351–363.
15. Chang CL, Fogler HS. Peptization and coagulation of asphaltenes in apolar media using oil-soluble polymers. *Fuel Sci Technol Int.* 1996;14:75–100.
16. Pillon LZ. Effect of dispersants and flocculants on the colloidal stability of asphaltenes. *Petroleum Sci Technol.* 2001;19:863–873.
17. Pedersen KS, Ronningsen HP. Influence of wax inhibitors on wax appearance temperature, pour point, and viscosity of waxy crude oils. *Energy Fuels.* 2003;17:321–328.
18. Guo XH, Adamson DH, Tinsley J, Pethica BA, Huang JS, Prud'homme RK. Synthesis of poly(ethylene-butene) random copolymers with hydroxylic grafts and effect of polar groups on deposition of wax and asphaltenes from crude oil. *Prepr Pap-Am Chem Soc Div Pet Chem.* 2004;49:272–273.
19. Kay PJ, Kelly DP, Milgate GI, Treloar FE. The conformational transition in poly(methacrylic acid) and butyl vinyl ether/maleic anhydride copolymer studied by  $^1\text{H}$  NMR linewidth measurements. *Macromol Chem Phys.* 1976;177:885–893.
20. Komber H. The  $^1\text{H}$  and  $^{13}\text{C}$  NMR spectra of alternating isobutene/maleic anhydride copolymer and the corresponding acid and sodium salt—a stereochemical analysis. *Macromol Chem Phys.* 1996;197: 343–353.
21. Bortel E, Styslo M. On the structure of radically obtained maleic anhydride/c4-alkene copolymers. *Macromol Chem Phys.* 1988;189: 1155–1165.
22. John J, Tang J, Yang ZH, Bhattacharya M. Synthesis and characterization of anhydride-functional polycaprolactone. *J Polym Sci A: Polym Chem.* 1997;35:1139–1148.
23. Tinsley JF, Prud'homme RK, Guo XH, Adamson DH, Callahan S, Amin D, Shao S, Krigel RM, Saini R. Novel laboratory cell for fundamental studies of the effect of polymer additives on wax deposition from model crude oils. *Energy Fuels.* 2007;21:1301–1308.
24. Tinsley JF, Prud'homme RK. Deposition apparatus to study the effects of polymers and asphaltenes upon wax deposition. *J Petrol Sci Eng.* 2010;72:166–174.
25. Li L, Guo XH, Adamson DH, Pethica BA, Huang JS, Prud'homme RK. Flow improvement of waxy oils by modulating long-chain paraffin crystallization with comb polymers: an observation by X-ray diffraction. *Ind Eng Chem Res.* 2011;50:316–321.
26. Chang CL, Fogler HS. Stabilization of asphaltenes in aliphatic solvents using alkylbenzene-derived amphiphiles. 1. Effect of the chemical structure of amphiphiles on asphaltene stabilization. *Langmuir.* 1994;10:1749–1757.
27. Chang CL, Fogler HS. Stabilization of asphaltenes in aliphatic solvents using alkylbenzene-derived amphiphiles. 2. Study of the asphaltene–amphiphile interactions and structures using Fourier transform infrared spectroscopy and small-angle X-ray scattering techniques. *Langmuir.* 1994;10:1758–1766.
28. Garcia MC. Crude oil wax crystallization. The effect of heavy *n*-paraffins and flocculated asphaltenes. *Energy Fuels.* 2000;14: 1043–1048.
29. Leon O, Contreras E, Rogel E, Dambakli G, Espidel J, Acevedo S. The influence of the adsorption of amphiphiles and resins in controlling asphaltene flocculation. *Energy Fuels.* 2001;15:1028–1032.

Manuscript received Jan. 2, 2011, and revision received May 11, 2011.